This article was downloaded by:
On: *22 January 2011*
Access details: *Access Details: Free Access*
Publisher *Taylor & Francis*
Informa Ltd Registered in England and Wales Registered Number: 1072954 Registered office: Mortimer House, 37-41 Mortimer Street, London W1T 3JH, UK

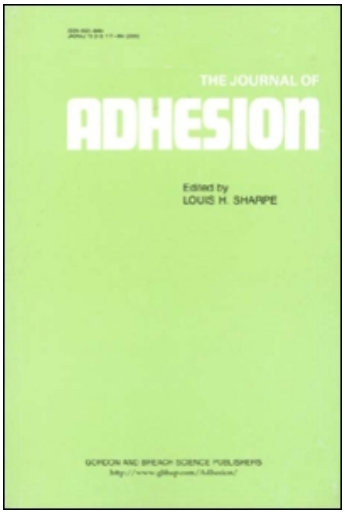

The Journal of Adhesion
Publication details, including instructions for authors and subscription information:
http://www.informaworld.com/smpp/title~content=t713453635

The Use of a Modified Mixed Mode Bending Test for Characterization of Mixed-mode Fracture Behavior of Adhesively Bonded Metal Joints

Z. Liu[a]; R. F. Gibson[a]; G. M. Newaz[a]
[a] Advanced Composites Research Laboratory, Department of Mechanical Engineering, Wayne State University, Detroit, Michigan, USA

Online publication date: 08 September 2010

To cite this Article Liu, Z. , Gibson, R. F. and Newaz, G. M.(2002) 'The Use of a Modified Mixed Mode Bending Test for Characterization of Mixed-mode Fracture Behavior of Adhesively Bonded Metal Joints', The Journal of Adhesion, 78: 3, 223 — 244
To link to this Article: DOI: 10.1080/00218460210408
URL: http://dx.doi.org/10.1080/00218460210408

PLEASE SCROLL DOWN FOR ARTICLE

Full terms and conditions of use: http://www.informaworld.com/terms-and-conditions-of-access.pdf

This article may be used for research, teaching and private study purposes. Any substantial or systematic reproduction, re-distribution, re-selling, loan or sub-licensing, systematic supply or distribution in any form to anyone is expressly forbidden.

The publisher does not give any warranty express or implied or make any representation that the contents will be complete or accurate or up to date. The accuracy of any instructions, formulae and drug doses should be independently verified with primary sources. The publisher shall not be liable for any loss, actions, claims, proceedings, demand or costs or damages whatsoever or howsoever caused arising directly or indirectly in connection with or arising out of the use of this material.

The Journal of Adhesion, 78: 223–244, 2002
Copyright © 2002 Taylor & Francis
0021-8464/02 $12.00 +.00

THE USE OF A MODIFIED MIXED MODE BENDING TEST FOR CHARACTERIZATION OF MIXED-MODE FRACTURE BEHAVIOR OF ADHESIVELY BONDED METAL JOINTS

Z. Liu, R. F. Gibson, and G. M. Newaz
Advanced Composites Research Laboratory,
Department of Mechanical Engineering,
Wayne State University, Detroit,
Michigan, USA

This paper summarizes recent mixed-mode I and II fracture experiments on adhesively bonded metal joints using a modified mixed-mode bending (MMB) test fixture and double cantilever beam (DCB)-type specimens. The MMB test had been previously developed and used for mixed-mode I and II delamination testing of composite laminates, but in the present research it is adapted and modified for fracture testing of adhesively bonded joints with metallic adherends. Strain energy release rates were evaluated by the use of improved analytical models. Mixed-mode fracture behavior of AA5754-0 aluminum alloy specimens bonded with a tough one-part epoxy adhesive (Dow Automotive Betamate 4601®) was characterized.

Keywords: Adhesively bonded metal joints; Mixed-mode bending test; Fracture behavior; Strain energy release rate; Fracture toughness; Fracture modes and mechanisms.

Downloaded At: 09:26 22 January 2011

INTRODUCTION

The automotive industry has considerable interest in the use of adhesively bonded joints for lightweight vehicle structures. Adhesively bonded joints enable design engineers to reduce weight, improve vehicle noise, vibration and harshness (NVH) performance, join

Received 16 December 2000; in final form 22 October 2001.

Presented at the 23rd Annual Meeting of The Adhesion Society, Inc., held at Myrtle Beach, South Carolina, USA, 20–23 February 2000.

The authors gratefully acknowledge the financial support of the Ford University Research Program and the technical advice and assistance of Carl Johnson, Matt Zaluzec, John Hill and Kim Lazarz of the Ford Research Laboratory.

Address correspondence to Ronald F. Gibson, Department of Mechanical Engineering, Wayne State University, 5050 Anthony Wayne Drive, Detroit, MI 48202, USA. E-mail: gibson@eng.wayne.edu

dissimilar materials and eliminate unattractive fastener holes in customer-visible areas [1].

In practice, crack growth in such adhesively bonded structures rarely occurs under pure mode I or mode II loading conditions, and a mixture of mode I and mode II loading conditions is more likely. It is important to develop reasonable and feasible methods to characterize the mixed mode fracture behavior of adhesive joints over the full range of mode mixity ratios from pure Mode I to pure Mode II, including the intermediate mode mixity ratios.

In this research, the Mixed Mode Bending (MMB) test fixture for composite delamination testing [2–3] was modified for fracture testing of adhesively bonded joints with metallic adherends by using a new load introduction concept and a new specimen design. AA5754-0 aluminum alloy specimens bonded with a tough one-part epoxy adhesive (Dow Automotive Betamate 4601®) were evaluated with the adhesive thickness 0.254 mm. Based on the experiments and improved analytical models, the mixed-mode fracture toughnesses and fracture mechanisms at different mode mixity ratios have been evaluated and investigated.

Downloaded At: 09:26 22 January 2011

MODIFICATIONS OF MMB FIXTURE AND SPECIMENS

The original MMB test fixture [2–3] was developed for the measurement of interlaminar fracture toughness of composite laminates under combined mode I and mode II loading conditions. The double cantilever beam (DCB)-type specimen geometry is simple and can be used for both mode I and mode II testing as well as for the mixed-mode I and II bending test. The conventional methods of load introduction normally used for the composite delamination specimens are piano hinges and end blocks. During the MMB tests of adhesively bonded aluminum joints with the original MMB fixture and specimen design (Figure 1), however, a number of difficulties such as extensive adherend yielding, hinge failure, hinge misalignment, true and theoretical loading point offset and ball bearing failure became evident. Therefore, in order to improve the MMB test accuracy, repeatability and reliability for adhesive joints with metallic adherends, a new load introduction concept had to be developed to overcome the problems mentioned above.

In order to minimize yielding in the adherends prior to crack growth, thick backing beams and a secondary adhesive bond were used in the modified fixture as shown in Figure 2. In this case, thin sheet material was the only form of the AA5754-0 aluminum adherend that was readily available. If thick adherends are available, of course there is no need for backing beams. The original piano hinge

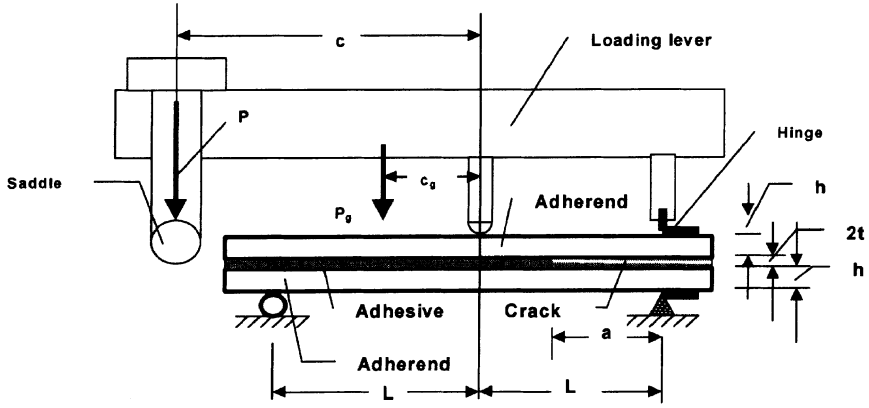

FIGURE 1 Original mixed-mode bending (MMB) test apparatus for adhesively bonded metal specimens.

Downloaded At: 09:26 22 January 2011

structures were replaced with clevis pin structures (Figure 2). The clevis pin structures are easy to assemble, and the holes in the backing beam were drilled with high precision to ensure the accuracy of pin alignment. In addition, the clevis pin structures locate the true loading center very close to the midplane of the specimen. Thus, the true and theoretical centers of rotation of adherends are identical, which is the basic assumption in beam theory and is critical for relatively large

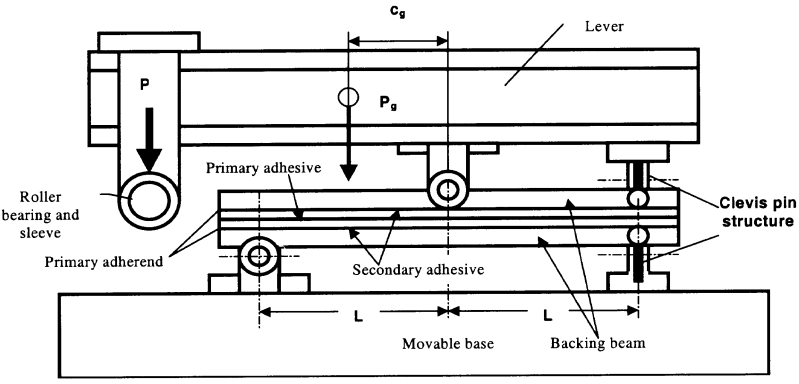

FIGURE 2 Modified MMB test fixture and specimen.

displacements. The other important thing is that the new load introduction fixture will not stiffen the test specimen as end blocks do. Furthermore, the ball bearings have been replaced by roller bearings and adapter sleeves (Figure 3), which make it possible to apply greater mixed mode loading which is required with the backing beam.

ANALYTICAL ASPECTS

Using the MMB apparatus, the load applied to the specimens can be decomposed into mode I (double cantilever beam, or DCB test) and mode II (end notched flexure, or ENF test) loading (Figure 4). Mode I and mode II loads P_I and P_{II}, respectively, are given by equations relating the applied load P to P_I and P_{II} [4, 7].

In order to evaluate mixed mode I and II fracture toughness more accurately from the MMB test data, improved analytical models have been developed using Timoshenko beam theory and including the adhesive layer effect from an elastic foundation analysis, as well as Saint-Venant end effects [5–7]. The mode I and mode II energy release rates can be calculated using the following equations [5–7]:

$$G_I = \frac{P_I^2}{2B}\left\{\frac{4}{E_F B(h+t)^3\lambda^3}\left[6\lambda^3 a^2 + 12\lambda^2 a + 6\lambda\right] + \frac{2}{\mu G_T B h} + \frac{48\chi a}{E_F B(h+t)^3}\right\} \tag{1}$$

$$G_{II} = \frac{1}{2}\frac{P_{II}^2}{2B}\{\Sigma_1 + \Sigma_2\} + \frac{3P_{II}^2\chi a}{B^2 E_F h^3} \tag{2}$$

$$\Sigma_1 = \frac{-3L^2 + 3a^2}{8E_F B(h+t)^3} - \frac{1}{4\mu G_T B(h+t)} \tag{3}$$

$$\Sigma_2 = \left[\frac{3L^2 + 15a^2}{8E_F^{\text{adherend}} B h^3} + \frac{2}{4\mu G_T^{\text{adherend}} B h}\right] \tag{4}$$

where G_I and G_{II} are the mode I and mode II energy release rates, respectively, and E_F and G_T are the effective flexural modulus and effective shear modulus of the uncracked part of the specimen, respectively [5, 7]. E_T^{adherend} and G_T^{adherend} are flexural modulus and shear modulus, respectively, of the cracked part of the specimen, μ is shear correction factor, $5/6$. B is the width of the specimen, λ and χ are

Downloaded At: 09:26 22 January 2011

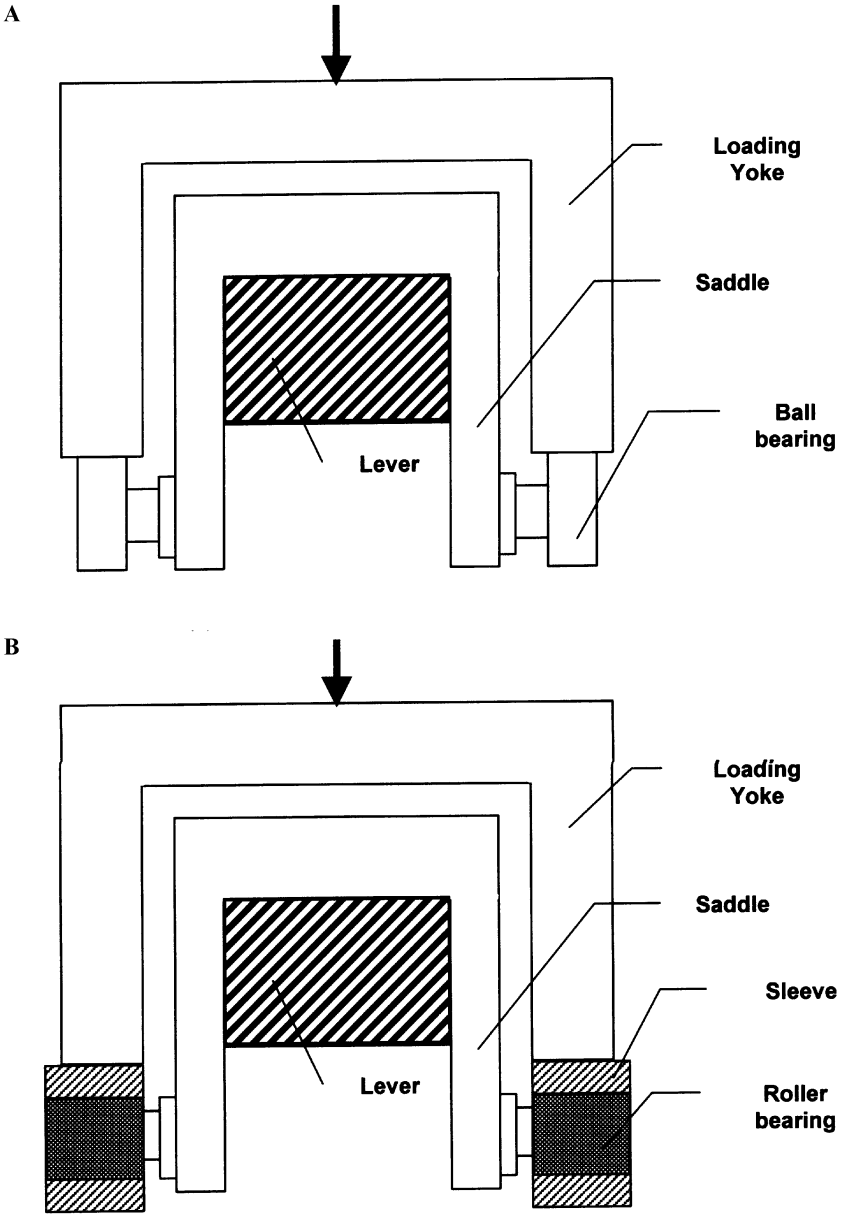

FIGURE 3 Modifications of MMB loading fixture. (a) The original MMB test fixture. (b) Modified MMB test fixture.

Downloaded At: 09:26 22 January 2011

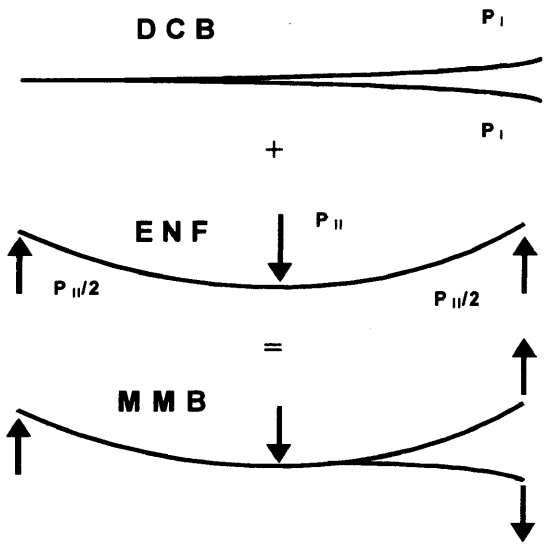

FIGURE 4 Separation of mode loadings in the MMB test.

Downloaded At: 09:26 22 January 2011

material and geometric parameters [5, 7], and L, a, h and t are described in Figures 1 and 2.

The mode I and mode II components of the mixed mode fracture energy, G_{IC}^m and G_{IIC}^m, can be evaluated using Equations (1) and (2) by replacing P_I and P_{II} with the corresponding critical values of those loads for crack growth. The total mixed mode fracture energy, G_C^m, is given by

$$G_C^m = G_{IC}^m + G_{IIC}^m \tag{5}$$

where the superscript m denotes a mixed mode fracture energy.

EXPERIMENTS

Materials, Specimen Fabrication, and MMB Test

Dow Betamate 4601, a one-part epoxy which contains glass beads with nominal 0.254 mm diameter was used for bonding and adhesive layer thickness control between two flat, 152.4 mm long, 25.4 mm wide, 1 mm thick aluminum alloy AA5754-0 adherends. The initial crack was formed by inserting Teflon film between the aluminum alloy AA5754-0 adherend and the Betamate 4601 adhesive layer. In order to avoid yielding of the thin aluminum AA5754-0 adherends, thicker aluminum

alloy 6061 backing beams (152.4 mm in length, 6.85 mm in thickness and 25.4 mm in width) were bonded to the aluminum alloy AA5754-0 adherends using Betamate 4601. The bond thickness between the 6061 and AA5754-0 layers was 0.25 mm. The adhesively bonded joints were cured in an oven at $180\,^{\circ}\mathrm{C} \pm 0.5\,^{\circ}\mathrm{C}$ for 40 minutes. During the adhesive curing process, a 280 mm $\times$ 105 mm $\times$ 25 mm thick steel plate was used as a weight on the specimens being cured in order to achieve uniform bonding quality. After curing, the specimen edges were polished using a file prior to testing and this, combined with the orange color of the adhesive, made the observation of the crack tip region possible without the need for any other crack tip location enhancing procedures such as the use of typewriter correction liquid.

No surface preparation was used on the aluminum alloy AA5754-0 adherends in order to simulate the manufacturing process used in the automotive industry. However, the bonding surfaces between the 6061 backing beams and the AA5754-0 adherends were polished with successively finer-grit sand papers, and were cleaned using 50:50 isopropyl alcohol.

The load was applied *via* an EnduraTec Smart Test servo-pneumatic testing machine operating in displacement control (Figure 5). Each specimen was loaded at a constant displacement rate of 0.002 in/sec

Downloaded At: 09:26 22 January 2011

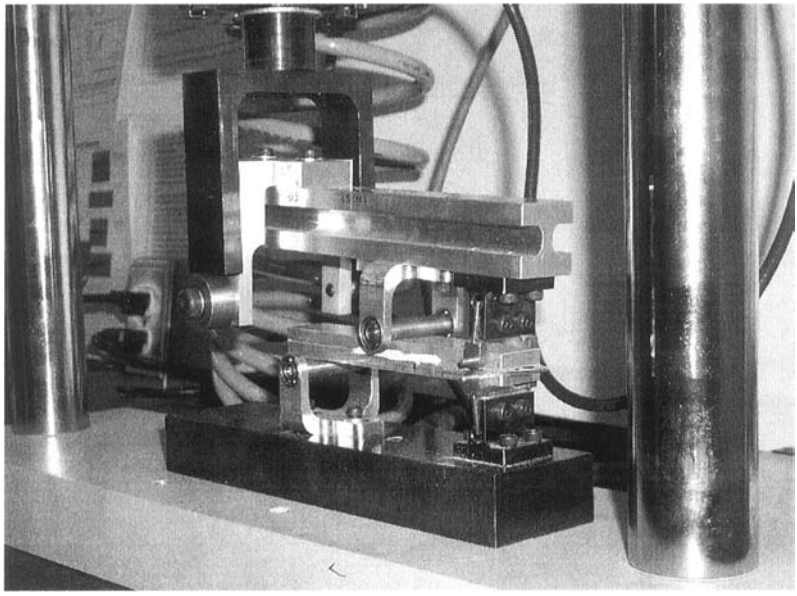

FIGURE 5 MMB test fixture and Enduratec machine.

(0.05 mm/sec) to a specific displacement. The critical load, which was used to evaluate the mixed-mode fracture energy, was determined once noticeable crack growth occurred. Once the crack started to grow, the displacement was then held constant for 5 seconds while the crack arrested. Following arrest, the new crack length was measured and the specimen was partially unloaded before reloading. The crack propagation was monitored by using an optical microscope with magnification up to 10X. At least two specimens were tested for each load condition.

The specimen span was 120 mm in the MMB tests. Mixed-mode fracture tests were conducted using four different lever lengths 100 mm, 60 mm, 50 mm and 35 mm to produce a range of mode mixity ratios. The specimen length was 152.4 mm in the DCB tests, while the span length in the ENF tests was 112.0 mm.

Downloaded At: 09:26 22 January 2011

RESULTS AND DISCUSSION

Analysis of Load-Displacement Curves

Figures 6(a–f) show the typical load-displacement curves which progressively change from the pure mode I loading condition to pure mode II loading condition as the lever length is reduced. It is interesting to see that at each loading condition the load increases continually from the point of crack initiation until the maximum load is reached, at which point the load starts to decrease with a slope. There was no sharp drop in the load, however. The slope of the load decrement becomes more pronounced as the mode II component is increased. When the G_I/G_{II} is about 1.0:1.0 (the lever length is equal to 50.0 mm) (Figure 6(d)), a slight instability of crack growth was noticed after the crack initiation. When G_I/G_{II} was about 0.4 (the lever length is equal to 35.0 mm), catastrophic crack growth took place after a very brief crack initiation (Figure 6(e)). This is a characteristic of the crack growth instability phenomenon, which means a more substantial participation of mode II (Figure 6(f)).

Figure 6 shows essentially linear load-displacement responses until the onset of crack propagation during loading, except that the first load-displacement response shows slight nonlinearity during loading due to the effect of preloading. It is also seen that there was significant permanent deformation of the MMB specimen after the test was completed. However, only the first $2 \sim 4$ loading-unloading loops, which only showed small amounts of plastic deformation after unloading, were used in the fracture toughness estimation. Based on these observations and considerations, it is believed that Linear Elastic

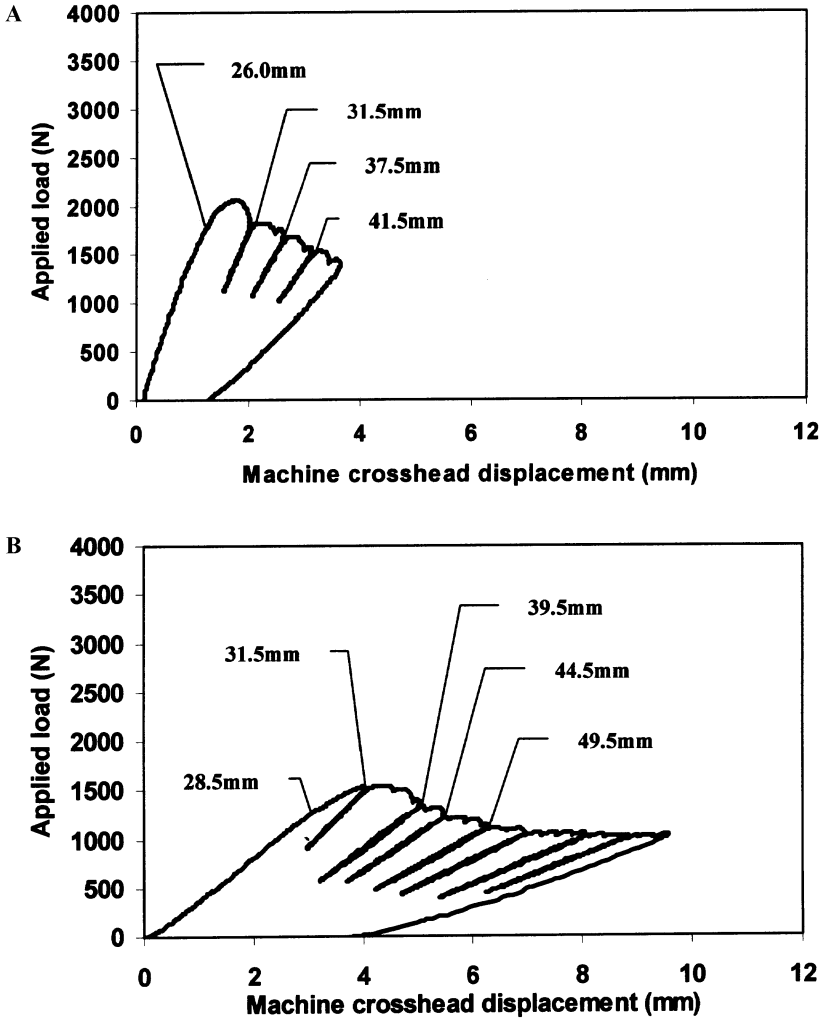

FIGURE 6 Typical load-displacement curves for MMB aluminum alloy AA5754-0/Dow Betamate 4601® specimens with 0.254 mm adhesive layer thickness. (a) Initial crack length: 26.0 mm; Pure mode I loading, (b) Initial crack length: 28.5 mm; Lever length: 100.0 mm, (c) Initial crack length: 26.5 mm; Lever length: 60.0 mm, (d) Initial crack length: 27.0 mm; Lever length: 50.0 mm, (e) Initial crack length: 25.0 mm, Lever length: 35.0 mm, (f) Initial crack length: 30 mm; span: 112 mm; pure mode II loading.

Fracture Mechanics (LEFM) is applicable to these adhesively bonded metal joints under mixed-mode loading. Nonlinear behavior may be attributed not only to the development of plastic deformation, but to

Downloaded At: 09:26 22 January 2011

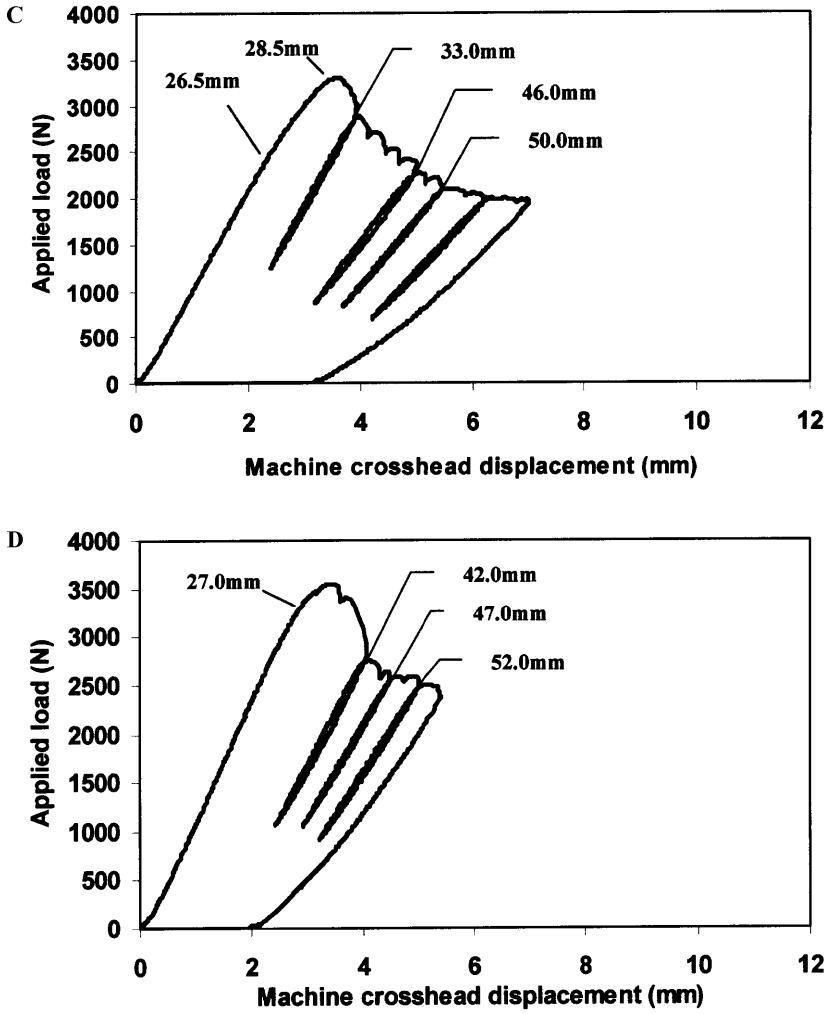

FIGURE 6 (*continued*)

crazing and microcracking in the adhesive layer ahead of the crack tip. It was noted that a small amount of subcritical crack growth took place before the cracks became unstable. From the toughness levels and the microcracking events that are described in Figure 7, it is more likely that there was resistance curve behavior where stable growth precedes unstable growth. This phenomenon was possibly due to resistance curve behavior which may be associated with such effects as changing state of stress and readjustment of the initial crack surfaces.

Downloaded At: 09:26 22 January 2011

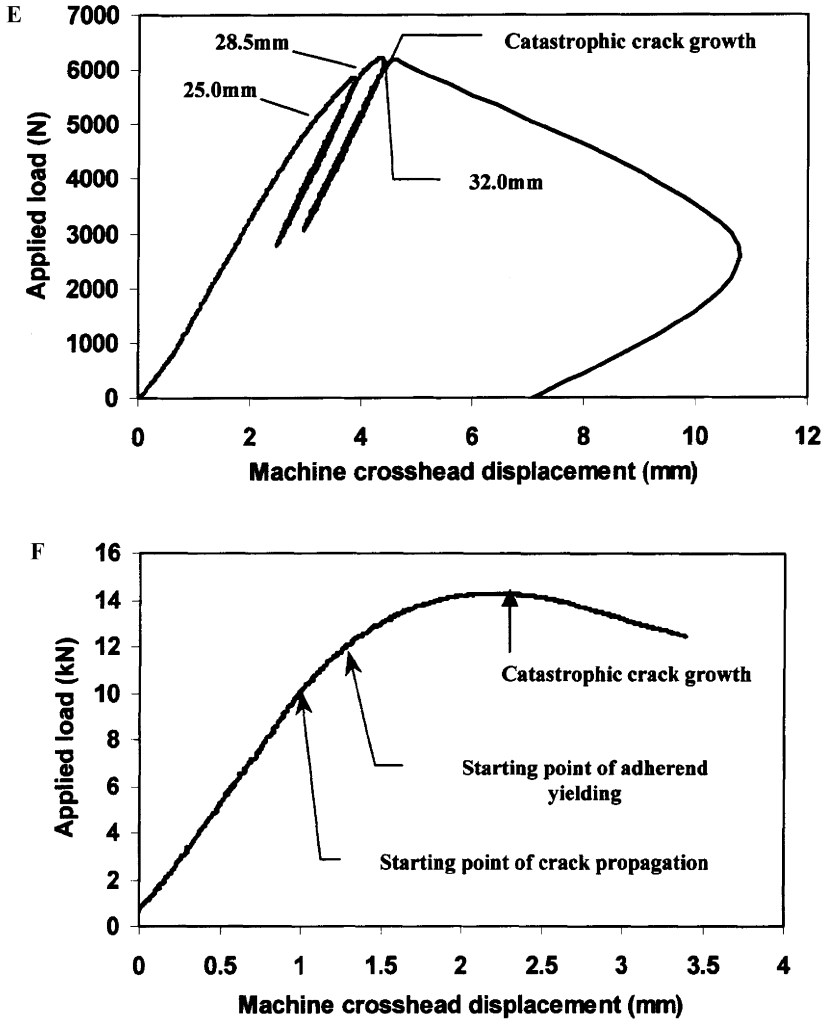

FIGURE 6 (*continued*)

Fracture Modes and Mechanisms

Figures 7(a–f) shows the microcrack growth mechanisms from pure mode I loading to pure mode II loading as well as four different mode mixities, and these figures correspond to the load-displacement curves for the same conditions in Figures 6(a–f). The failure modes in the MMB tests were basically (visually) interfacial. But for the pure mode I loading condition, the failure mode was cohesive, and the crack

Downloaded At: 09:26 22 January 2011

Downloaded At: 09:26 22 January 2011

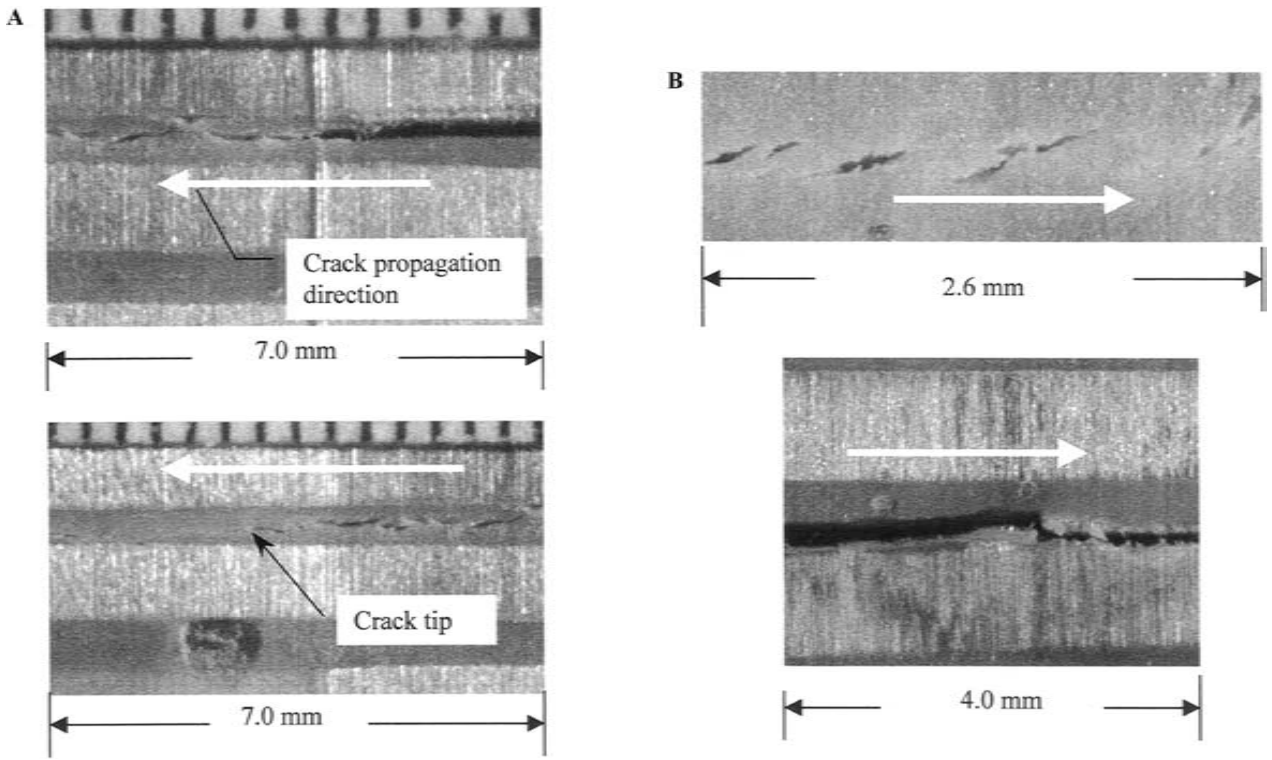

FIGURE 7 Crack growth mechanisms for MMB aluminum alloy AA5754-0/Dow Betamate 4601® specimens with 0.254 mm adhesive layer thickness. (a) Pure mode I loading, (b) L = 60 mm, c = 100 mm, (c) L = 60 mm, c = 60 mm, (d) L = 60 mm, c = 50 mm, (e) L = 60 mm, c = 35 mm, (f) pure mode II loading.

Downloaded At: 09:26 22 January 2011

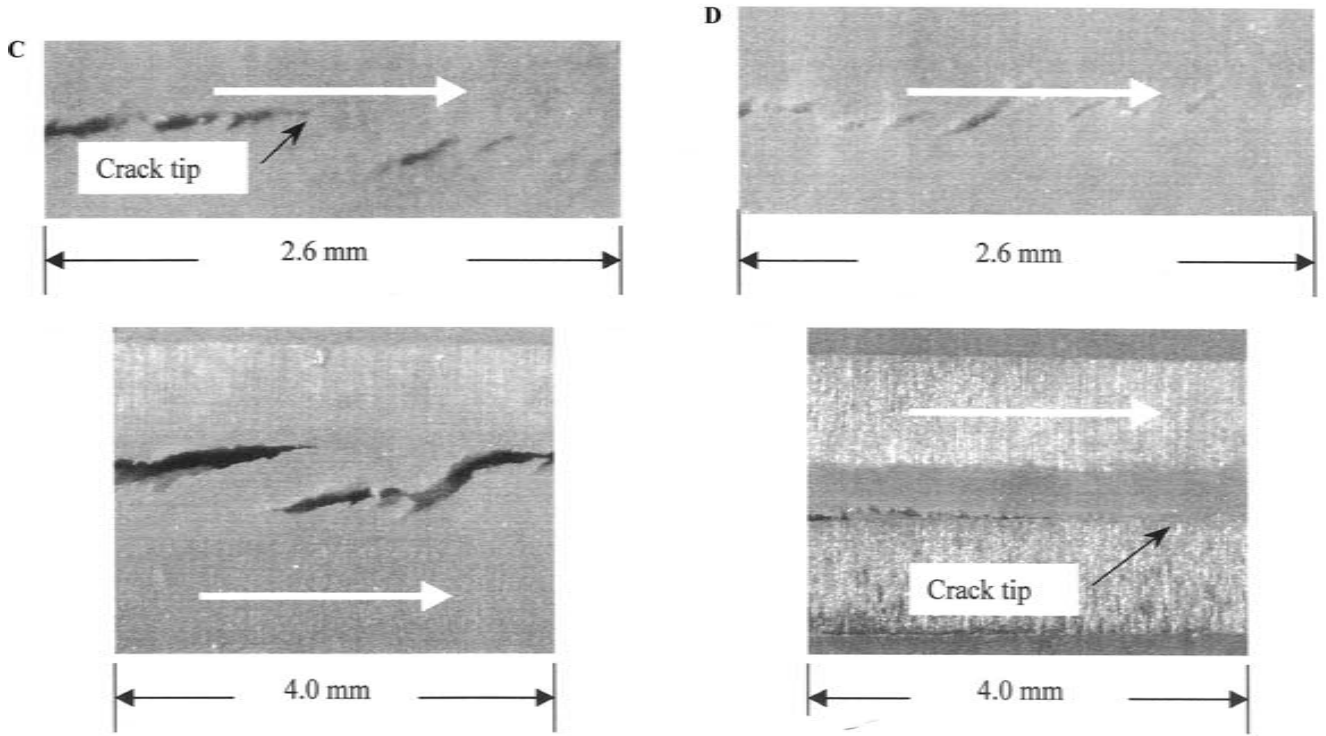

FIGURE 7 (*continued*)

Downloaded At: 09:26 22 January 2011

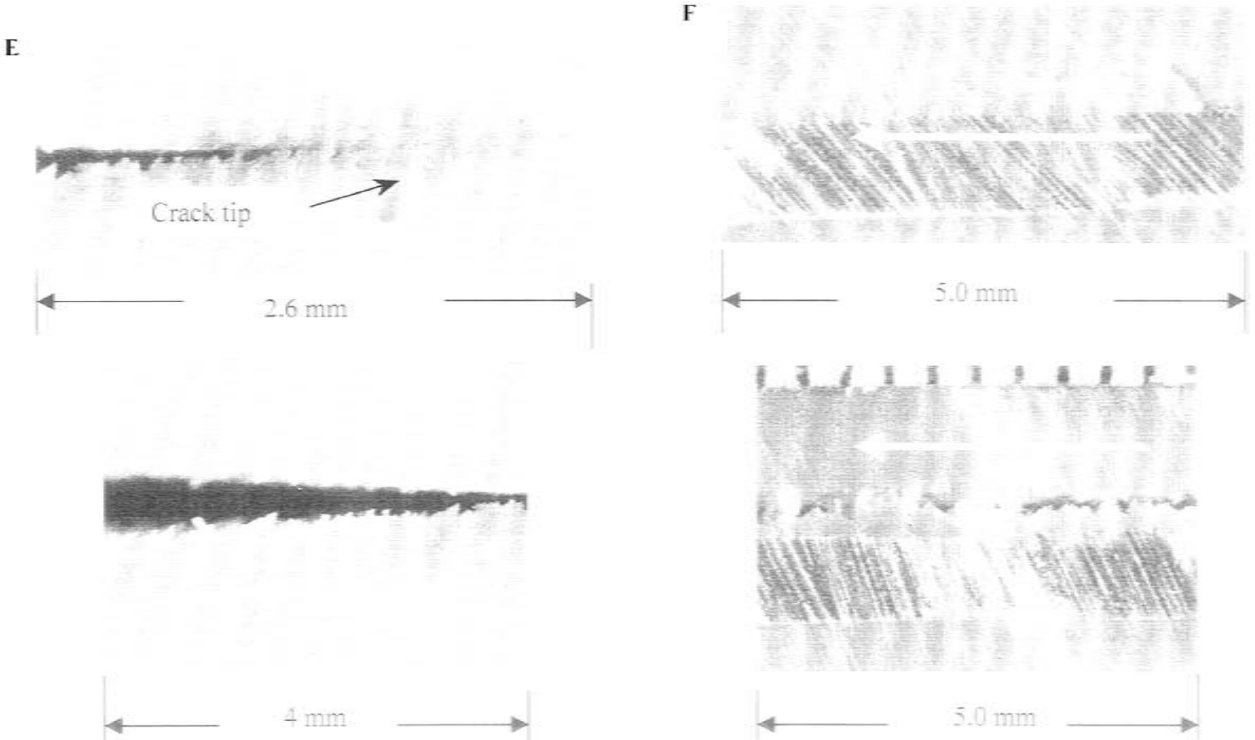

FIGURE 7 (*continued*)

surface was a serrated interfacial failure along the subinterfacial location parallel to the interface at the mode II loading condition. It was observed in the experiments that the crack growth was preceded by whitening or crazing of the adhesive ahead of the main crack tip, and the crazing was then followed by the initiation and growth of microcracks. The adhesive crazing ahead of the main crack tip took place very often around the glass beads and voids. The propagation of the main crack occurred by linking the main crack tip with the closest microcrack ahead of the crack tip. The orientation of the microcracks varied with loading conditions, from about $\theta = 0^\circ$ from the longitudinal axis of the specimen (Figure 8) for pure mode I DCB specimens, to about $\theta = 45^\circ$ for Mode II ENF specimens. This is because the crack surface is generally perpendicular to the maximum tensile normal stress, and the maximum tensile normal stress or principal stress in the adhesive varies from the vertical direction for pure mode I to $\theta = 45^\circ$ from the vertical for pure mode II. The fracture surfaces for mode II looked much rougher than those of other loading conditions (Figure 7).

Downloaded At: 09:26 22 January 2011

Fracture Toughness and Fracture Envelope

The material properties used in the evaluation of fracture energy are listed in Table 1.

In the calculation of the mode I fracture energy, the stiffness of the elastic foundation is the combined stiffness of the fraction of the Betamate 4601 adhesive layer below the fracture surface, K_1^{4601}, the adhesive layer between backing beam and the adherend, K_2^{4601}, the backing beam (aluminum 6061 sheet), K_{6061}, and adherend (aluminum AA5754-0 sheet), K_{5754}, which are assumed to act as springs in series, *i.e.*,

$$\frac{1}{K} = \frac{1}{K_{6061}} + \frac{1}{K_{5754}} + \frac{1}{K_1^{4601}} + \frac{1}{K_2^{4601}} \tag{6}$$

The mixed-mode fracture toughness is calculated by using Equation (5).

Figure 9 shows the variation of fracture toughness with crack length for pure mode I and three different mixed-mode conditions for the adhesive layer thickness of 0.254 mm. The variation of fracture toughness with crack length for pure Mode II ENF specimens was not available due to insufficient data. It can be seen from Figure 9 that the fracture toughness is almost constant for crack lengths less than $0.75L$, where L was the half span of the specimen. However, the fracture toughness increases when the crack length is greater than

Downloaded At: 09:26 22 January 2011

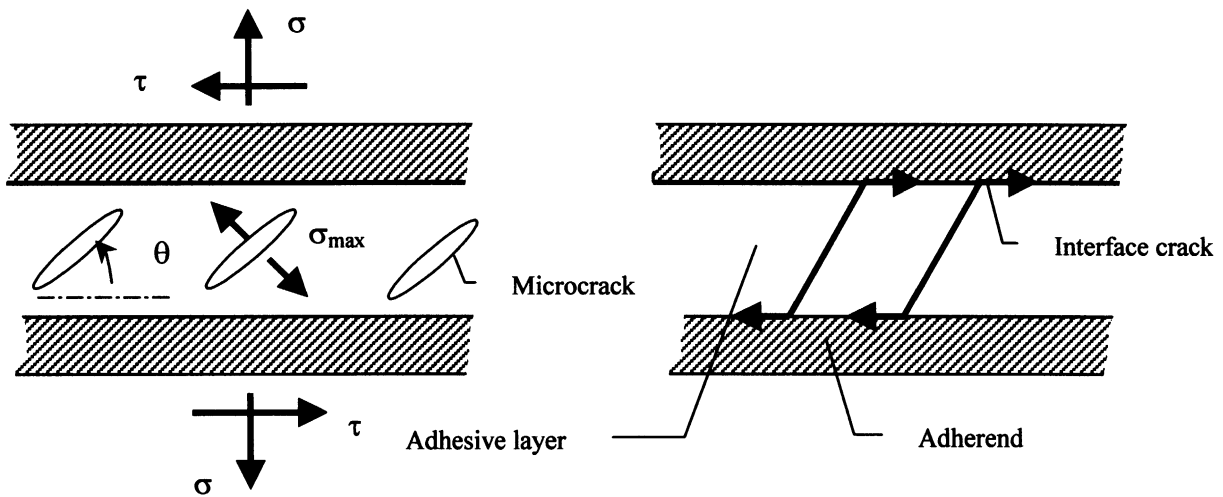

FIGURE 8 Schematic illustration of the orientation of microcracks.

TABLE 1 Material Properties for MMB Specimens

	Young's modulus GPa	Poisson's ratio
Al 6061	68.95	0.30
AA5754-0	68.95	0.30
Dow Betamate 4601	3.80	0.36

$0.75L$. It was observed in the experiments that the crack propagation is very slow and crack extension is very small when a/L approaches 0.75. It seems that there may be interaction between the crack tip stress field and the stress field from the central loading point.

The averaged fracture toughnesses at three different mixed-mode loading conditions as well as pure mode I and pure mode II loading conditions for two adhesive layer thicknesses are listed in Table 2. The values for adhesive layer thickness of 0.254 mm indicate that the mode I and mixed-mode fracture toughnesses are almost the same, but the mode II toughness is somewhat higher. However, a slight decrement of fracture toughness compared with mode I fracture toughness for some intermediate mode mixities ($c = 100.0$ mm and $c = 50.0$ mm) was noted. The main reason is believed to be that the microcracks extended to the interfaces between the adherends and adhesive layer before linking (Figures 7 and 8), while the microcracks under mode I loading condition did not extend to the interfaces. It is noted that the total mixed mode fracture toughness had some scatter, but was basi-

Downloaded At: 09:26 22 January 2011

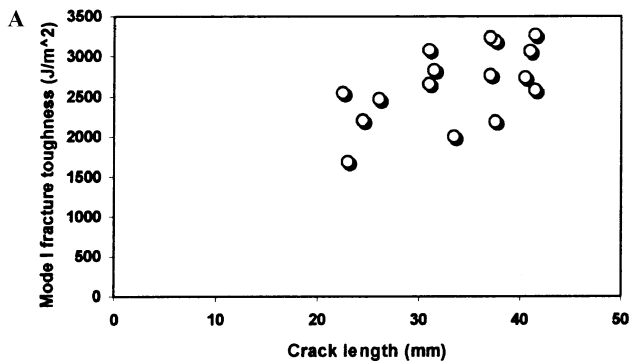

FIGURE 9 Variation of fracture toughness with crack length. Bonding thickness is 0.254 mm. (a) Pure mode I loading, (b) mixed-mode loading, lever length: 100.0 mm, (c) mixed-mode loading, lever length: 60.0 mm, (d) mixed-mode loading, lever length: 50.0 mm.

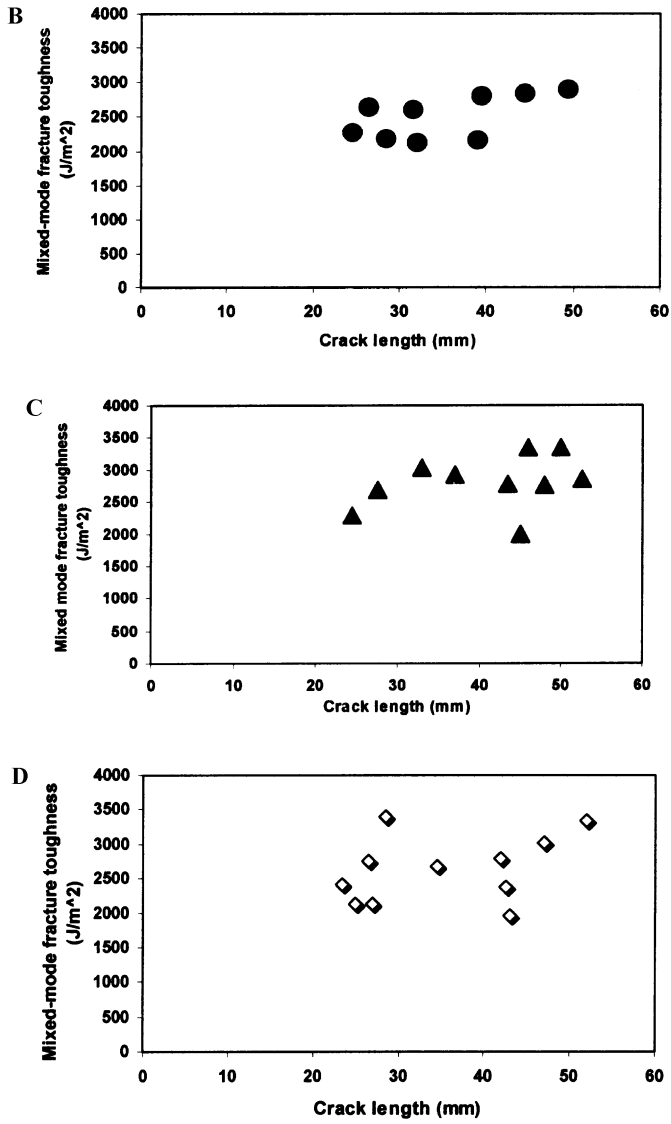

FIGURE 9 (*continued*)

cally independent of mode mixity ratios, and the average total mixed mode fracture toughness is between $2.5\,KJ/m^2$, and $2.8\,KJ/m^2$.

The results of the tests with the DCB, MMB and ENF specimens with adhesive layer thickness of 0.254 mm are summarized in the

Downloaded At: 09:26 22 January 2011

TABLE 2 Averaged Toughnesses at Different Loading Conditions for AA5754-0/Betamate 4601® Joints

Loading condition	Fracture toughness (J/m^2) (adhesive layer thickness: 0.254 mm)
Mode I	2657.1
C = 100 mm	2498.8
C = 60.0 mm	2797.9
C = 50.0 mm	2629.4
Mode II	3227.5

fracture envelopes shown in Figure 10. It can be concluded from Figure 10 that for the adhesive layer thickness of 0.254 mm the data may be approximated by the equation

$$\frac{G_I^m}{G_{IC}} + \frac{G_{II}^m}{G_{IIC}} = 1 \tag{7}$$

There are several possible reasons for the data scatter and the sensitivity to crack length. Following the automotive industry practice, no surface preparation was used for the primary adherends, and this is believed to be a significant cause of data scatter. In this work, only $3 \sim 4$ specimens were used for each loading condition, and more specimens are needed for each loading condition. The Teflon film was used to create the initial crack. However, after the specimen was cured at high temperature, the edges of the specimen had to be polished and the initial crack had to be reopened slightly using a razor blade. This may have caused a very slight crack propagation which is difficult to observe by using an optical microscope with the 10X magnification.

Downloaded At: 09:26 22 January 2011

Comparison of Adhesively Bonded Joints

Table 3 summarizes some mode I and mode II fracture energy values for various combinations of adhesives and adherends including the adhesive studied in this research and others from literature.

As shown in Table 3, the mode I fracture energy of the aluminum alloy AA5754-0/Dow Betamate 4601 joints without surface preparation is only slightly lower than that of aluminum alloy/XD 4600 joint with grit-blasted and degreased surface preparation. Compared with other adherend/adhesive joints, the Dow Betamate 4601 adhesive appears to be a very tough adhesive [8–14].

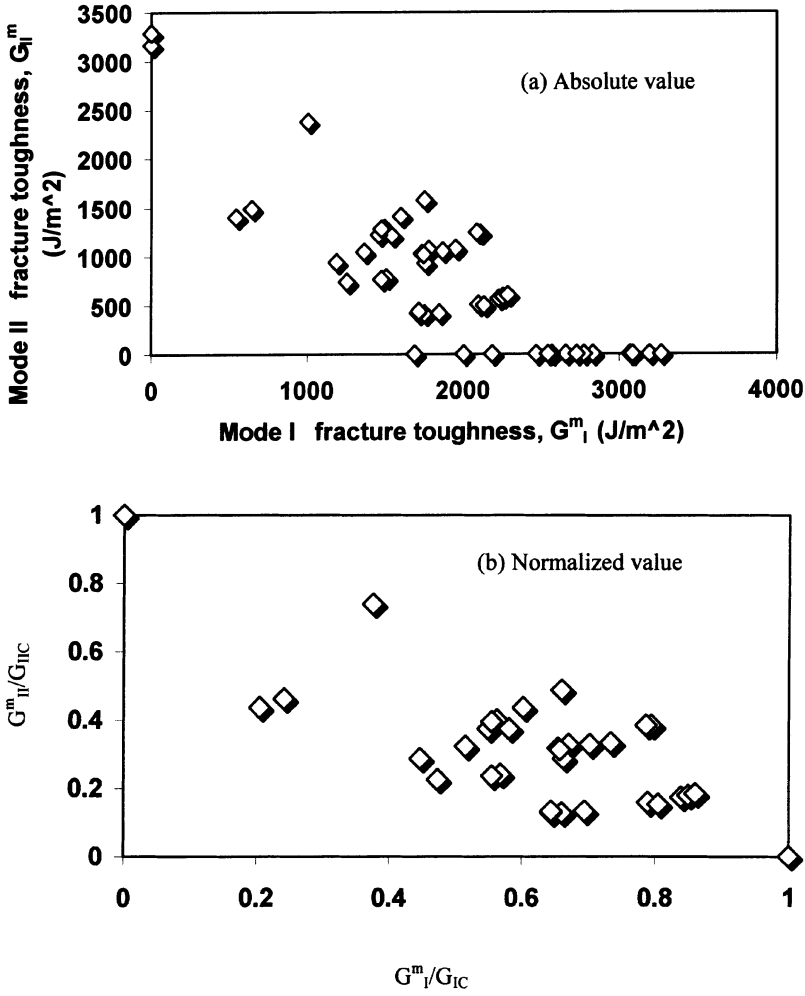

FIGURE 10 Fracture toughness envelope of adhesive Betamate 4601®: Adhesive layer thickness is 0.254 mm.

CONCLUSIONS

A MMB test fixture and specimen configuration for mixed mode composite delamination testing has been successfully modified for mixed mode fracture testing of adhesively bonded specimens with metallic adherends. Within the constraints of no surface preparation and a small number of specimens, the modified MMB test fixture and specimens gave reasonably reliable and consistent results. The results

Downloaded At: 09:26 22 January 2011

TABLE 3 Summary and Comparison of Fracture Toughnesses for Mode I and Mode II for Various Joints

Adhesives and manufacturer	Adherend materials	G_{IC} (J/m^2)	G_{IIC} (J/m^2)
Epoxy Cybond 4523GB® (American Cyanamid) [8]	7075-T6 aluminum	212	575
Permabond Esp 310® (American Cyanamid) [9]	7075-T6 aluminum	794	5605
FM 300K.05® (American Cyanamid) [10]	7075-T651 aluminum alloy	654	–
FM 300 (American Cyanamid) [11]	Aluminum-alloy	1120	1400
Ferokal 4520-34® (Teroson) [12]	EG steel	740	–
XD 4600 (Ciba Polymers) [12]	Aluminum-alloy (chromic-acid etch)	3500 ± 125	–
XD 4600 (Ciba Polymers) [12]	Aluminum-alloy (grit-blasted and degreased)	3000 ± 65	–
XD 4600 (Ciba Polymers) [13]	Aluminum-alloy	$2400 \sim 2800$	–
LMD 1141® (Ciba-Geigy) [13]	Steel	$3700 \sim 4700$	–
Urethane (Ashland Company) [14]	Glass fiber reinforced composites	1800	6000
Epoxy (Goodrich) [14]	Glass fiber reinforced composites	4000	4000
Dow Betamate 4601® (Essex Specialty Products, Inc.)*	Aluminum alloy 5754 (no surface preparation)	2657.1	3228.5
Dow Betamate 4601 (Essex Specialty Products, Inc.)*	Aluminum alloy 5754 (no surface preparation)	2498 ~ 2798 (mixed-mode I and II)	

* From current research.

show that the variations of mixed mode fracture energy with crack length and mode mixity ratios can be measured using the modified MMB fixture and improved analytical models.

REFERENCES

[1] Cornille, H. J., Weishaar, J. C. and Young, C. S., "The P2000 Body Structure," SAE Technical Paper, No. 982405 (1998).

[2] Reeder, J. R. and Crews, Jr., J. H., "Mixed-Mode Bending Method for Delamination Testing," *AIAA Journal*, **28**(7), 1270–1276 (1990).

Downloaded At: 09:26 22 January 2011

[3] Reeder, J. R. and Crews, Jr., J. H., "Redesign of the Mixed-mode Bending Delamination Test to Reduce Non-linear Effects," *J. Composites Technology and Research*, **14**, 12–19 (1992).
[4] Bhashyam, S. and Davidson, B. D., "Evaluation of Data Reduction Methods for the Mixed Mode Bending Test," *AIAA J.*, **35**(3), 546–552 (1997).
[5] Liu, Z. Y., Gibson, R. F., and Newaz, G., "Improved Analytical Model for Mode I Energy Release Rate in Adhesively Bonded DCB Specimens," *Proceedings of 31st International SAMPEE Technical Conference*, Chicago, IL, 568–580 (1999).
[6] Liu, Z. Y., Gibson, R. F., and Newaz, G., "Mixed-mode Fracture Behavior of Adhesively Bonded Joints in Automotive Industry," *Proceedings of 23rd Annual Meeting of the Adhesion Society*, Myrtle Beach, SC, 19–21 (2000).
[7] Liu, Z. Y., "Characterization of the Mixed-mode Fracture Behavior of Adhesively Bonded Metal Joints for Automotive Vehicle Structures," Ph.D. Dissertation, Wayne State University (2000).
[8] Fernlund, G. and Spelt, J., "Mixed-mode Fracture Characterization of Adhesive Joints," *Composites Science and Technology*, **50**, 441–449 (1994).
[9] Papini, M., Fernlund, G. and Spelt, J. K., "Effect of Crack-Growth Mechanism on the Prediction of Fracture Load of Adhesive Joints," *Composites Science and Technology*, **52**, 561–570 (1994).
[10] Ripling, E. J., Crosley, P. B. and Johnson, W. S., "A Comparison of Pure Mode I and Mixed-mode I–III Cracking of an Adhesive Containing an Open Knit Cloth Carrier," *Adhesively Bonded Joints: Testing, Analysis and Design*, ASTM STP, **981**, Johnson, W. S., Ed. (American Society for Testing and Materials, Philadelphia, 1988), pp. 163–182.
[11] Liechti, K. M. and Freda, T., "On the Use of Laminated Beams for the Determination of Pure and Mixed-Mode Fracture Properties of Structural Adhesives," *J. Adhesion*, **29**, 145–169 (1989).
[12] Jethwa, J. K. and Kinloch, A. J., "The Fatigue and Durability Behavior of Automotive Adhesives: Part 1. Fracture Mechanics Tests," *J. Adhesion*, **61**, 71–95 (1997).
[13] Kinloch, A. J., Blackman, B. R. K., Taylor, A. C., and Wang, Y., "The Failure of Adhesively Bonded Joints Under High Rates of Deformation," In: *Proceedings of Euradh '96: Adhesion '96 Conference*, pp. 467–471 (Institute of Materials, London, 1996).
[14] Swadener, J. G., Liechiti, K. M. and Liang, Y. M., "Mixed-mode Fracture Automotive Bonded Joints," *SAMPE-ACCE-DOE Advanced Composites Conference*, September 27–28, Detroit, 367–370 (1999).

Downloaded At: 09:26 22 January 2011